Polymer Bulletin (2023) 80:13051–13068
https://doi.org/10.1007/s00289-023-04684-x

ORIGINAL PAPER

Experimental investigation of absorption shielding efficiency of rubber composites

Ján Kruželák[1,2,3] · Andrea Kvasničáková[1] · Klaudia Hložeková[1] · Rastislav Dosudil[2] · Marek Gořalík[3] · Ivan Hudec[1]

Received: 14 June 2022 / Revised: 11 November 2022 / Accepted: 9 January 2023 /
Published online: 26 January 2023

Abstract

Manganese–zinc ferrite, nickel-zinc ferrite and the combination of both fillers were used for fabrication of composites. Then, carbon black was applied in combination with ferrites in the second type of composites. The main goal was to investigate the influence of fillers on absorption shielding efficiency and physical–mechanical properties of composites. It was revealed that incorporation of ferrites into rubber matrix leads to fabrication of composites that are able to absorb electromagnetic radiation. The higher was the amount of nickel-zinc ferrite in fillers combinations, the higher was the absorption shielding performance of composites. The results showed that nickel-zinc ferrite demonstrated better absorption shielding potential. The absorption shielding efficiency of composites filled with carbon black and ferrites was lower when compared to equivalent composites filled only with ferrites, which can be attributed to higher electrical conductivity of composites due to the presence of carbon black. On the other side, the incorporation of carbon black caused the improvement in physical–mechanical properties of composites, mainly the enhancement of the tensile strength, modulus and hardness.

Keywords Rubber · Magnetic soft ferrites · Carbon black · Shielding · Absorption

✉ Ján Kruželák
jan.kruzelak@stuba.sk

[1] Department of Plastics, Rubber and Fibres, Faculty of Chemical and Food Technology, Slovak University of Technology in Bratislava, Radlinského 9, 812 37 Bratislava, Slovakia

[2] Department of Electromagnetic Theory, Faculty of Electrical Engineering and Information Technology, Slovak University of Technology in Bratislava, Iľkovičova 3, 812 19 Bratislava, Slovakia

[3] Centre of Polymer Systems, University Institute, Tomas Bata University in Zlín, třída Tomáše Bati 5678, 760 01 Zlín, Czech Republic

Introduction

The increasing demand for informatization and industrialization in today`s modern society is strongly connected with implementation of new and modern electronic concepts. However, this is also strongly connected with higher accumulation of electromagnetic radiation in the surrounding. This electromagnetic radiation is often termed as electromagnetic interference (EMI). EMI can be defined as a phenomenon where one electromagnetic field interferes with another, which results in distortion of both fields. It can negatively influence the functionality of electronic devices, even might cause their malfunction [1, 2]. It has also been reported harmful effect of electromagnetic radiation on the health conditions of human beings. The most common symptoms are headaches, irritability, insomnia, fatigue, failure of attentions, which may result in more serious illnesses [3, 4]. EMI has thus become a serious problem and the need for electromagnetic radiation shielding has been more and more pronounced over last decades. The total effectiveness of shielding can be understood as the sum of reflection, absorption and multiply reflection of EMI. The shielding by reflection increases with the increase of materials conductivity and is preferred mainly for highly conductive materials, like metals [5]. However, shielding by reflection causes reflected radiation to interfere with other electronic sources thus resulting in secondary EMI effect. The materials with electric and magnetic dipoles are good candidates for shielding by absorption [6, 7]. To such materials belong some iron based oxides or magnetic soft ferrites. The absorbed energy is then transferred to another form of harmless energy, as for instance to heat. For this reason, the absorption shielding is much more preferred in comparison with reflection shielding. The third mechanism of shielding is multiply reflection, which can be defined as reflection of EMI from surfaces and phase interfaces within the shield. Typically, materials with good ability of multiply reflection are composites with fillers having high specific surface area or large phase interface, as for instance carbon based fillers like carbon nanofibers, carbon nanotubes, or graphene nanoplatelets [8].

Polymer matrices are mostly electrically and magnetically non-conductive and thus they cannot shield electromagnetic radiation. However, the shielding performance to polymer matrices can be imparted by incorporation of suitable fillers. The most popular filler for polymer, mostly rubber matrices is carbon black due to low cost, easy production and adjustable physical properties. For specific applications, as for EMI shielding, other fillers have also been incorporated into polymer formulations, as for example metal powders, metal oxides, ferrites or other types of carbon-based fillers (graphite, graphene, carbon nanofibers or carbon nanotubes) [5, 9–13]. Each of the mentioned filler can provide shielding effects to polymer matrices. The intensity of shielding and the type of shielding mechanism (reflection, absorption, multiply reflection) depend mainly on the nature and structure of the filler and radiation frequency. A lot of the studies have been focused on testing of shielding effects of polymer composites filled with carbon based fillers at high electromagnetic frequencies, mostly within the *X*-band ranges (8.2–12.4 GHz) or even within higher radiation frequencies [14–18]. The results

revealed that those composites are able to efficiently shield electromagnetic radiation at high frequencies. However, the shielding performance of composites filled with carbon based fillers seems to be poorer at low frequencies and is often based primarily on reflection of EMI. As already mentioned, shielding by reflection is undesirable due to secondary interference of reflected radiation with initial radiation emitted from other electronic sources, thus causing additional EMI effect. The commonly used electronic and electromagnetic devices (TV sets, computers, radios, etc.) operate at lower frequencies, usually up to 3–4 GHz. Thus, from practical point of view, the shielding of EMI at low frequencies is of high importance. The results of our previous experiments revealed that for absorption shielding at low frequencies, magnetic soft ferrites are suitable fillers for rubber composites. In addition to laboratory prepared manganese–zinc ferrites and lithium ferrites [19, 20], commercially obtained manganese-zinc ferrite has been tested [21, 22]. The experimental outputs demonstrated that the application of manganese-zinc ferrite into rubber compounds results in fabrication of composites that can shield electromagnetic radiation by absorption mechanisms. Magnetic filler was incorporated into rubber matrix in concentration scale ranging from 100 to 500 phr. It was shown that with increase in filler content, the absorption maxima and absorption shielding effectiveness were more pronounced at lower frequencies of electromagnetic radiation. It was also found out that the highest absorption shielding performance exhibited composites filled with 200 and 300 phr of the filler. Thus, in the present work, the content of magnetic fillers was kept on constant level − 300 phr. In addition to manganese–zinc ferrite, commercially available nickel–zinc ferrite with similar structural characteristics, and combination of both fillers in acrylonitrile-butadiene rubber were tested for EMI absorption shielding. Then, carbon black was dosed to rubber compounds in constant amount and the influence of the applied fillers on absorption shielding ability and physical–mechanical properties of composites was investigated.

Experimental

Materials

Manganese–zinc ferrite MnZn and nickel–zinc ferrite NiZn in powder form were provided by Epcos s.r.o., Czech Republic. Both fillers represent magnetic soft ferrites with spinel structure and similar particle size distribution. Although the total particle size distribution is relatively wide, most particles for both fillers ranged from 10 to 30 μm.

Table 1 Structural characteristics of ferrites

Filler	Particle size distribution (μm)	D10 (μm)	D50 (μm)
MnZn	0.7–50	4.7	16.3
NiZn	0.2–70	3.0	21.4

Table 2 Composition of composites filled with ferrites in phr and their designation

NBR	100	100	100	100	100
ZnO	3	3	3	3	3
Stearic acid	2	2	2	2	2
CBS	1.5	1.5	1.5	1.5	1.5
Sulfur	1.5	1.5	1.5	1.5	1.5
MnZn ferrite	300	200	150	100	0
NiZn ferrite	0	100	150	200	300
Designation	Mn300	Mn200 Ni100	Mn150 Ni150	Mn100 Ni200	Ni300

Table 3 Composition of composites filled with carbon black and ferrites in phr and their designation

NBR	100	100	100	100	100
ZnO	3	3	3	3	3
Stearic acid	2	2	2	2	2
CBS	1.5	1.5	1.5	1.5	1.5
Sulfur	1.5	1.5	1.5	1.5	1.5
Carbon black	25	25	25	25	25
MnZn ferrite	300	200	150	100	0
NiZn ferrite	0	100	150	200	300
Designation	CB-Mn300	CB-Mn200 Ni100	CB-Mn150 Ni150	CB-Mn100 Ni200	CB-Ni300

The average particle size distribution of both fillers with values D10 a D50 are mentioned in Table 1. Parameters D10 a D50 represent percentage of particles with diameters lower than the given value. D50 can be defined as median showing that 50% of particles is lower than roughly 16 μm for MnZn ferrite and roughly 21 μm for NiZn ferrite. Special type of conductive carbon black CB having trademark VULCAN® XC 72 was supplied from Cabot Corporation, USA. Acrylonitrile-butadiene rubber NBR provided by Sibur International, Russia (SKN 3345, content of acrylonitrile 31–35%) served as rubber matrix. Cross-linking of rubber composites was performed by application of sulfur curing system consisting of stearic acid and zinc oxide (Slovlak, Košeca, Slovakia) as activators, *N*-cyclohexyl-2-benzothiazole sulfenamide CBS (Duslo, Šaľa, Slovakia) as accelerator and sulfur (Siarkopol, Tarnobrzeg, Poland) as curing agent (Tables 2 and 3). The used semi-EV curing system consisting of roughly equivalent sulfur to accelerator ratio provides composites with good compromise between physical–mechanical characteristics and resistance to thermo-oxidative ageing. The used chemicals in the work were of technical grade with high purity.

Methods

Fabrication of composites

Two types of rubber composites were fabricated and tested in the study. In the first type of composites, manganese–zinc ferrite, nickel–zinc ferrite and combination of both fillers were incorporated into NBR based matrix. The total content of magnetic fillers was kept on constant level − 300 phr. The composite filled only with manganese–zinc ferrite was designated as Mn300, the composite filled only with nickel–zinc ferrite was marked as Ni300. The other three types of composites were designated according to mutual ratio of both fillers as shown in Table 2. The amount of curing additives was also constant in all composites. The second series of composites was fabricated with the same composition, moreover, carbon black as carbon-based filler was incorporated into rubber compounds in constant loading − 25 phr (Table 3).

Rubber, filler and curing additives were compounded in the chamber of tangential kneading equipment Bradender in two step mixing process. The temperature was set up to 90 °C and the speed of rotors was 55 rpm. First, rubber was plasticated for 2.5 min, then stearic acid and zinc oxide were added and after next two min, magnetic filler, or fillers were applied. The total time of first step mixing was 9 min. The rubber compounds were cooled down and calendered in two-roll mill. In the second step, sulfur together with accelerators were introduced and the compounding process continued for 4 min at 90 °C and 55 rpm. Final step was additional homogenization and sheeting of rubber compounds using two-roll mill. The preparation procedure of the second series rubber compounds was very similar, but rubber batch based on NBR and carbon black was pre-compounded using semi-industrial kneading machine Buzuluk. Then, the preparation procedure followed the same conditions as mentioned above. The curing process was performed at 160 °C and pressure of 15 MPa in a hydraulic press Fontijne following the optimum cure time of corresponding rubber compounds. After curing, thin sheets with dimensions 15 × 15 cm and thickness 2 mm were obtained.

Investigation of absorption shielding characteristics

The frequency dependencies of complex (relative) permeability $\mu = \mu' - j\mu''$ for toroidal samples were measured using combined impedance/network analysis method by means of a vector analyser (Agilent E5071C) in the frequency range of 1 MHz–6 GHz (Fig. 1). During measurements, a toroidal sample was inserted into a magnetic holder (Agilent 16454A) and the complex permeability was evaluated from measured impedances (Eq. 1):

$$\mu = \mu' - j\mu'' = 1 + (Z - Z_{air})/\left(jh\mu_0 f \ln(b/c)\right) \quad (1)$$

where Z and Z_{air} are the input complex impedances of the 16454A holder with and without a toroidal sample, respectively, h is the height of the sample, $\mu_0 = 4 \cdot 10^{-7}$

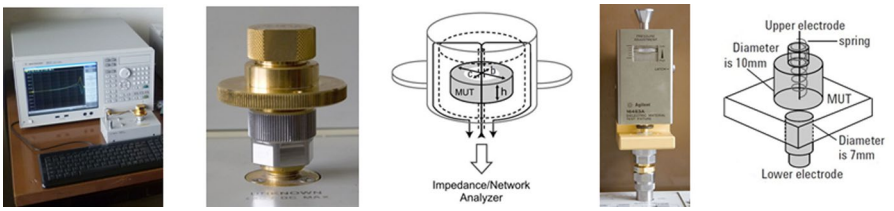

Fig. 1 From left to right: measurement set-up with Agilent E5071C network analyser, magnetic holder 16454A, a toroidal sample inserted into the holder, dielectric holder 16453A and its structure

H/m is the permeability of free space, f is the frequency, and b and c are the outer and inner diameters of the sample.

The frequency dependencies of complex (relative) permittivity $\varepsilon = \varepsilon' - j\varepsilon''$ for disc samples were measured using combined impedance/network analysis method by means of a vector analyser (Agilent E5071C) in the frequency range of 1 MHz–6 GHz (Fig. 1). During measurements, a disc sample was inserted into a dielectric holder (Agilent 16453A) and the complex permittivity was computed from measured admittance (Eq. 2):

$$\varepsilon = \varepsilon' - j\varepsilon'' = (Yh)/(jw\varepsilon_o S) \tag{2}$$

where Y is the input complex admittance of the 16453A holder with a disc sample, h is the height of the sample, $\varepsilon_0 = 8.854 \cdot 10^{-12}$ F/m is the permittivity of free space, and S is the area of lower electrode. In case of electrically conductive material with dc electrical conductivity σ_{dc}, the imaginary part of ε should be replaced by $\varepsilon'' - \sigma_{dc}/2\pi\varepsilon_o$. The electrical dc conductivity of composite materials was evaluated using standard two-probe method.

High frequency single-layer electromagnetic wave absorption properties (return loss RL, matching thickness d_m, matching frequency f_m, bandwidth Δf for RL at − 10 dB and RL at − 20 dB, and the minimum of return loss RL_{min}) of composite materials were obtained by calculations of return loss (Eq. 3):

$$RL = 20 \log \left| (Z_{in} - 1)/\left(Z_{in} + 1\right) \right| \tag{3}$$

where $Z_{in} = (\mu/\varepsilon)^{1/2} \tanh[(j\omega \cdot d/c)(\mu\varepsilon)]$ is the normalized value of input complex impedance of the absorber, d is the thickness of the single-layer absorber (backed by a metal sheet), c is the velocity of light in vacuum. The composite absorbs maximum of the electromagnetic plane wave energy when normalized value of impedance $Z_{in}1$. The maximum absorption is then reached at a matching frequency $f = f_m$, matching thickness $d = d_m$ and minimum return loss RL_{min}.

Determination of physical–mechanical properties

The tensile properties of composites were evaluated by using Zwick Roell/Z 2.5 appliance. The cross-head speed of the measuring device was set up to 500 mm/min and the tests were carried out in compliance with the valid technical standards.

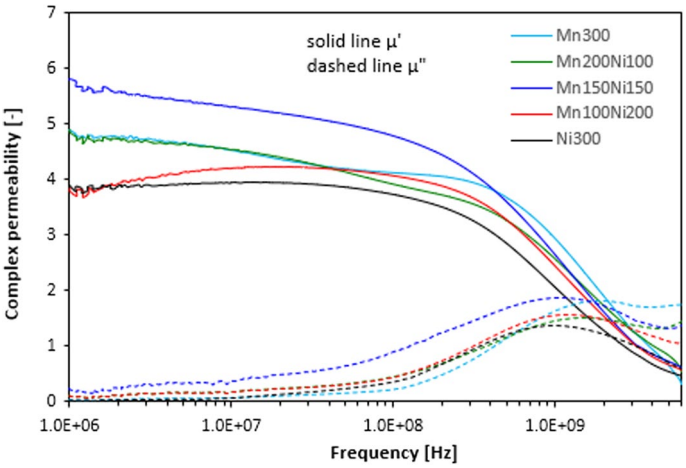

Fig. 2 Frequency dependences of complex permeability for composites filled with ferrites

Dumbbell-shaped test specimens (thickness 2 mm, length 80 mm, width 6.4 mm) were used for measurements. The hardness was measured by durometer and expressed in Shore A unit.

Results and discussion

Absorption shielding efficiency of composites

In the first part of the study, manganese–zinc ferrite, nickel–zinc ferrite and their combinations were incorporated into matrix based on NBR. The total content of fillers was kept on constant level − 300 phr. The man aim was to investigate the influence of magnetic soft ferrites on absorption shielding performance of rubber magnetic composites, which was characterized trough determination of return loss. Complex permittivity and complex permeability were first evaluated in frequency range from 1 MHz to 6 GHz. Due to the complexity of experimental procedure, the achieved results represent only one measurement for each sample.

From frequency dependences of complex permeability ($\mu = \mu' - j\mu''$) it is shown that the lowest real permeability μ' in the whole frequency range exhibited composite filled with nickel–zinc ferrite (Ni300) (Fig. 2). There was recorded almost no change of real part up to roughly 100 MHz, then it sharply decreased with increase in frequency (from $\mu' \sim 3.9$ in frequency interval 1 MHz–100 MHz to $\mu' = 0.5$ at 6 GHz). The highest real permeability at initial frequency was found to have the composite filled with combination of manganese–zinc ferrite and nickel–zinc ferrite in their equivalent ratio (Mn150Ni150). Differences in real permeability of composites filled with magnetic soft ferrites became less visible with increase in frequency. Real permeability of all composites decreased to very low values at a maximum frequency. The imaginary permeability μ'' seems to be frequency independent up about

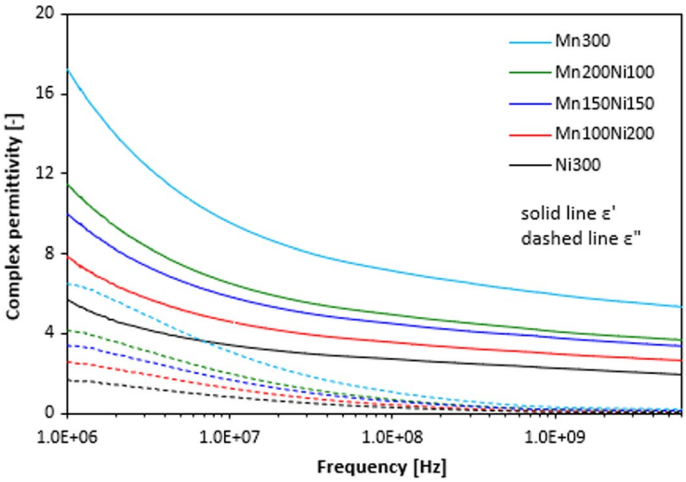

Fig. 3 Frequency dependences of complex permittivity for composites filled with ferrites

100 MHz. Then, it increased up to maximum at a resonance frequency (around 1 GHz) and dropped down. The maximum in $\mu''(f)$ dependences corresponds to the maximal permeability loss, or magnetic loss. The highest value of imaginary permeability seems also to have the composite filled with equivalent ratio of both ferrites. However, generally it can be stated that no significant changes of complex permeability were observed in dependence on the type of applied ferrite or ferrite combinations.

On the other hand, there was recorded clear dependence of complex permittivity ($\varepsilon = \varepsilon' - j\varepsilon''$) on the type of ferrite. From Fig. 3 it becomes apparent that the highest real permittivity was found to have the composite filled with manganese–zinc ferrite (Mn300), while the lowest one exhibited composite filled with nickel–zinc ferrite (Ni300). The biggest difference in ε' between both composites was observed at an initial frequency ($\varepsilon' = 17.2$ for Mn300 and $\varepsilon' = 5.7$ for Ni300). As also shown, the higher was the proportion of nickel–zinc ferrite in composites with fillers combinations, the lower was the real permittivity. The real permittivity of composites showed decreasing trend with increase in electromagnetic radiation frequency. With the rise in frequency, the differences in real permittivity became smaller. At a maximum frequency, the real permittivity of the composites MnZn300 and NiZn300 reached the value 5.3 and 1.96, respectively. The imaginary permittivity of composites was lower and followed the dependences in fillers composition. As seen, composite filled only manganese–zinc ferrite was found to have the highest ε'', while the lowest imaginary part demonstrated the composite filled with only nickel–zinc ferrite. The increase in frequency resulted in the decrease of imaginary permittivity up to about 1 GHz, then settled on a constant value with almost no dependence on the type of filler, or fillers combinations.

Based on known parameters, return loss *RL* in decibels unit were calculated. Return loss provide useful information about the amount of electromagnetic radiation that can be efficiently absorbed by the shielding material. Experimental

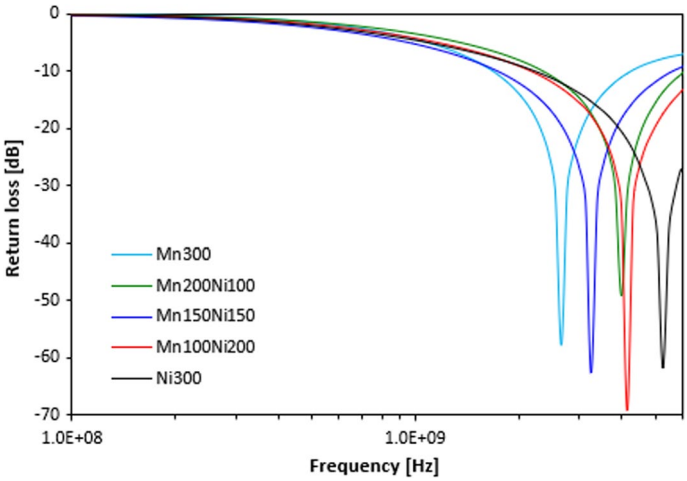

Fig. 4 Frequency dependences of return loss for composites filled with ferrites

Table 4 Electromagnetic absorption parameters of composites filled with ferrites

sample	RL_{min} (dB)	f_m (MHz)	Δf (MHz) – 10 dB	Δf (MHz) – 20 dB
Mn300	– 58	2660	2500	740
Mn200Ni100	– 49	3980	3600	1160
Mn150Ni150	– 63	3250	3800	1130
Mn100Ni200	– 69	4140	3800	1530
Ni300	– 62	5260	3750	2090

investigations have revealed that materials reaching return loss at − 10 dB are able to efficiently absorb roughly 90–95% of electromagnetic radiation. Return loss at − 20 dB relate to absorption of almost 99% EMI [23–25].

The frequency dependences of return loss for composites filled with magnetic soft ferrites are graphically illustrated in Fig. 4. The computed values of electromagnetic absorption characteristics, i.e. minimum value of return loss RL_{min} at a matching frequency f_m, matching frequency f_m and effective absorption bandwidth Δf for RL at − 10 dB and − 20 dB are summarized in Table 4. As shown in Fig. 4 and Table 4, with increasing content of nickel–zinc ferrite in fillers combination, the absorption maxima and absorption shielding effectiveness of composites shift to higher frequencies of EMI. The matching frequency for composite filled with manganese–zinc ferrite (Mn300) was 2660 MHz with the absorption maximum − 58 dB, while matching frequency for composite filled nickel–zinc ferrite (Ni300) was 5260 MHz with absorption maximum reaching − 62 dB. It also becomes apparent that composite filled with 300 phr of MnZn ferrite exhibited the lowest effective frequency bandwidth at − 10 and − 20 dB (RL at − 10 dB within 1700–4200 MHz frequency range and RL at − 20 dB within

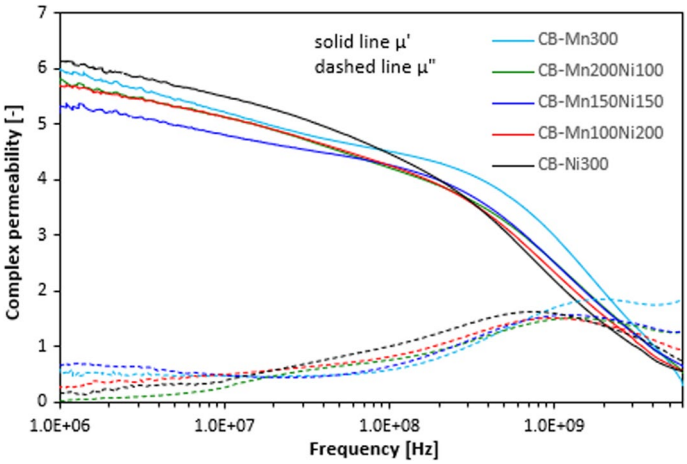

Fig. 5 Frequency dependences of complex permeability for composites filled with carbon black and ferrites

2320–3060 MHz frequency range), which means that this composite is the least effective for EMI absorption shielding. On the other hand, as the best absorption shielding material can be considered the composite loaded with 300 phr of nickel–zinc ferrite (Ni300) as it demonstrated return loss at − 10 dB and − 20 dB in the widest frequency range, i.e. from 2250 MHz to 6 GHz at − 10 dB and from 3910 MHz to 6 GHz at − 20 dB. It must be noted that due to the limitation of the used equipment and possibility to measure only up to 6 GHz, the effective absorption bandwidth for this composite would be much wider. In the case of composites filled with combinations of both fillers one can see that effective frequency ranges for absorption shielding at − 10 dB and − 20 dB become broader with the increased ratio of nickel–zinc ferrite. Based upon the achieved results it can be stated that all composites exhibit satisfactory absorption shielding ability as they reached return loss at − 10 dB and − 20 dB within wide frequency ranges. As the absorption shielding ability of composites increased with increasing content of nickel–zinc ferrite, it becomes clearly apparent that NiZn filler demonstrates better absorption shielding potential.

The next series of composites was fabricated with the same composition, but in addition carbon black was incorporated into rubber compounds in constant amount − 25 phr. The real permeability μ' of composites filled with carbon black and ferrites showed decreasing trend with increasing frequency (Fig. 5). More evident decrease was possible to observe from 100 MHz. The imaginary permeability μ'' was much lower than the real part at low frequencies, but the difference between both parts became smaller with the increase in frequency. As in the previous composite types, the influence of ferrites or ferrites combination on frequency behaviour of real μ' and imaginary permeability μ'' was low visible. The values of complex permeability for composites filled with carbon black and

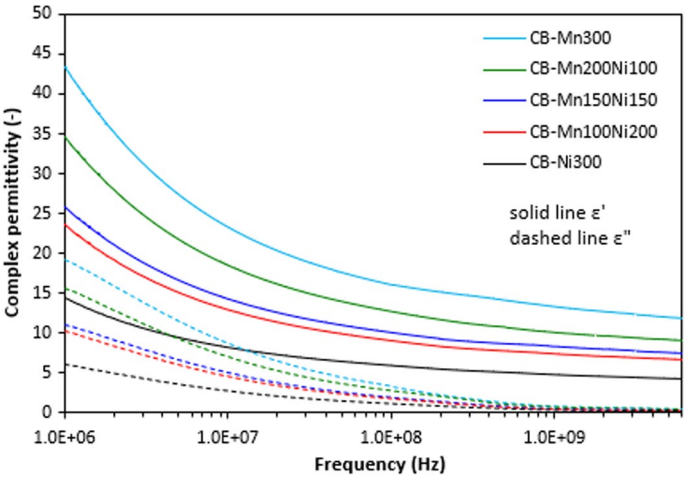

Fig. 6 Frequency dependences of complex permittivity for composites filled with carbon black and ferrites

ferrites were very similar to those for composites filled only with magnetic fillers with no clear influence of materials composition on μ' and μ''.

As seen in Fig. 6, the increase in frequency resulted in the decrease of both, real ε' and imaginary ε'' permittivity of composites. Imaginary permittivity was lower than the real part and decreased to very low values at about 1 GHz. With next increase in frequency, it settled almost on constant value. The highest real and imaginary permittivity demonstrated the composite filled with CB and manganese–zinc ferrite (CB-Mn300), while the lowest values of both parts was found to have the composite filled with nickel–zinc ferrite (CB-Ni300). Complex permittivity of composites filled with CB and ferrites combinations (CB-Mn200Ni100, CB-Mn150Ni150, CB-Mn100Ni200) was situated between the equivalent values of composites designated as CB-Mn300 and CB-Ni300. The higher was the amount of nickel–zinc ferrite if ferrites combination, the lower was the real and imaginary permittivity. When comparing Figs. 3 and 6, it becomes apparent that the real permittivity of composites filled with CB and ferrites was almost three times higher in comparison with composites filled only with magnetic fillers. The composite designated as CB-Mn300 exhibited real permittivity $\varepsilon' = 43.3$ at an initial frequency. Then, it decreased to almost 12 at 6 GHz. The real permittivity of the composite filled with CB and nickel–zinc ferrite (CB-Ni300) decreased from 14.3 to 4.3 by increase in frequency from 1 MHz to 6 GHz. The imaginary permittivity of composites with incorporated carbon black was also higher in comparison with composites filled with magnetic fillers at low frequencies, but the differences in ε'' for both composite types became negligible over 1 GHz.

The character of frequency dependences of return loss for composites filled with carbon black and magnetic fillers was very similar as for composites filled only with ferrites. As shown in Fig. 7 and Table 5, the composite CB-Mn300 showed the absorption maximum at the lowest frequency ($RL_{min} = -46$ dB at

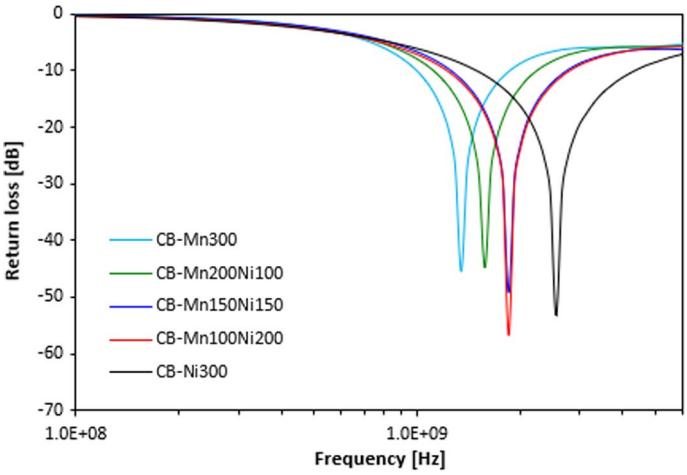

Fig. 7 Frequency dependences of return loss for composites filled with carbon black and ferrites

Table 5 Electromagnetic absorption parameters of composites filled with carbon black and ferrites

sample	RL_{min} (dB)	f_m (MHz)	Δf (MHz) – 10 dB	Δf (MHz) – 20 dB
CB-Mn300	−46	1347	860	250
CB-Mn200Ni100	−45	1581	1110	330
CB-Mn150Ni150	−49	1856	1470	430
CB-Mn100Ni200	−57	1856	1570	460
CB-Ni300	−54	2556	2800	770

$f_m = 1347$ MHz). This composite was also found to have the narrowest absorption frequency bandwidth at $RL = -10$ and -20 dB. It ranged between 1 GHz and 1860 MHz at -10 dB ($\Delta f = 860$ MHz) and from 1230 to 1480 MHz at -20 dB ($\Delta f = 250$ MHz). The increasing proportion of nickel–zinc ferrite resulted in the increase of frequency at which the composites exhibited maximum absorption shielding effectiveness and effective absorption frequency bandwidth became broader, too. As the best absorption shield can be marked the composite with designation CB-Ni300, as it can effectively absorb 90–95% of EMI from 1500 to 4300 MHz ($\Delta f = 2800$ MHz at $RL = -10$ dB) and almost 100% of EMI from 2200 MHz to almost 3 GHz ($\Delta f = 770$ MHz at $RL = -20$ dB). The absorption maximum of this composite was at -54 dB at frequency 2556 MHz. When comparing Figs. 4, 7 and Tables 4, 5 it becomes apparent that composites filled with CB and ferrites exhibited roughly one half lower matching frequencies f_m. They also provided higher values of return loss RL_{min} at matching frequencies and narrower absorption peaks. As seen in Tables 4 and 5, effective frequency bandwidths at -10 and -20 dB were roughly 2.5 or 3 times lower when compared to equivalent composites filled only with magnetic fillers. This means that the

incorporation of carbon black into composites led to the shifting of their absorption shielding efficiency to lower frequencies of EMI on one hand. On the other hand, it becomes clearly obvious that absorption shielding efficiency of composites based on CB and ferrites is lower, as an evidence of narrower absorption peaks. For better understanding of the fillers influence on absorption shielding efficiency, the electrical resistivity of composites was evaluated (electrical resistivity is a reciprocal value of electrical conductivity). From Fig. 8 it becomes apparent that electrical resistivity of composites filled only with ferrites is higher with almost no dependence on materials composition. The application of carbon black resulted in the decrease of electrical resistivity of composites, which means that composites with incorporated CB demonstrated higher electrical conductivity. Carbon based fillers, including carbon black, are characterized by unique electrical characteristics and thus the incorporation of CB into composites caused the increase in electrical conductivity. The electrical conductivity of CB and ferrites filled composites showed decreasing tendency with increasing proportion of nickel–zinc ferrite. The differences in electrical resistivity or electrical conductivity between both type composites became smaller with increasing proportion of nickel–zinc ferrite in magnetic fillers combination. Higher electrical conductivity of composites filled with CB and ferrites was reflected in their higher real permittivity and subsequently to higher complex permittivity. The highest real and imaginary permittivity, among all tested materials, were found to have composites filled with CB and manganese–zinc ferrite (CB-Mn300). Frequency dependences of permittivity are influenced not only by polarization mechanisms (polarization of the filler, rubber matrix and interfacial polarization) but also by higher conductivity of carbon black. The presence of conductive carbon black in the rubber matrix leads to the higher accumulation of electrical charges within the composites, but also contributes to higher filler-rubber interfacial charge polarization. This was subsequently reflected in higher values of permittivity of the equivalent composites. When comparing both types of tested ferrites, the achieved results

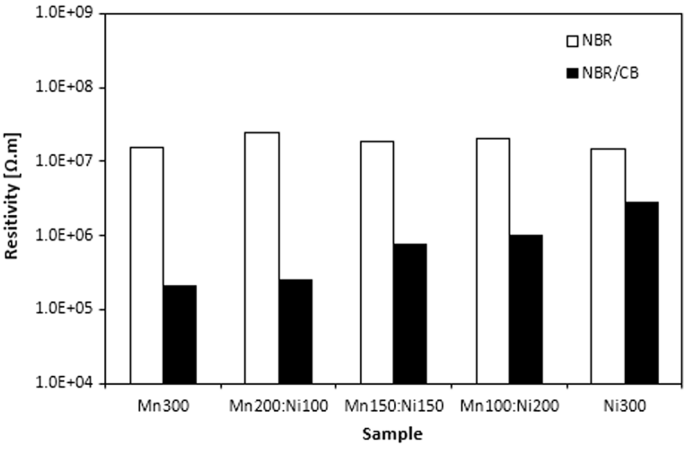

Fig. 8 Resistivity of composites filled with ferrites and composites filled with carbon black and ferrites

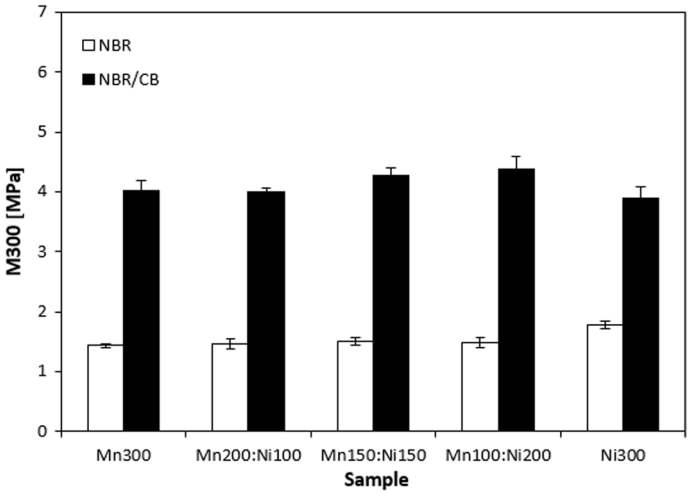

Fig. 9 Modulus M300 of composites filled with ferrites and composites filled with carbon black and ferrites

also point out to higher conductivity of manganese–zinc ferrite, although it was not experimentally confirmed by determination of electrical resistivity of composites filled only with magnetic fillers.

As it was already mentioned, composites filled with CB and ferrites demonstrated narrower absorption peaks and their absorption shielding ability shifted to lower frequencies in comparison with their equivalents filled only with magnetic fillers. Based on the achieved results it could be stated that electrical resistivity, or electrical conductivity is one of the crucial parameters affecting absorption shielding efficiency of composites, mainly at low frequencies. It becomes obvious that the higher is the electrical conductivity of composites, the poorer is their absorption shielding ability. Simultaneously, they can absorb EMI at lower frequencies. According to available literature sources, materials with higher electrical conductivity are more prone to shielding by reflection, mainly at low frequencies [26–28]. The obtained experimental outputs are in line those assumptions. Among all tested materials, composite filled with nickel–zinc ferrite (Ni300) exhibited the widest frequency absorption bandwidth at − 10 and − 20 dB, which suggests that it is the most effective absorber of electromagnetic radiation.

Physical–mechanical properties of composites

The values of physical–mechanical properties of composites are graphically illustrated in Figs. 9, 10, 11 and 12. They represent average value of five parallel measurements. It becomes apparent that the modulus M300 (Fig. 9) and tensile strength (Fig. 10) of composites filled with only with ferrites were low, which is in line with non-reinforcing character of magnetic fillers. Looking at Fig. 10 it is seen that the tensile strength of ferrites filled composites showed slight increasing trend with

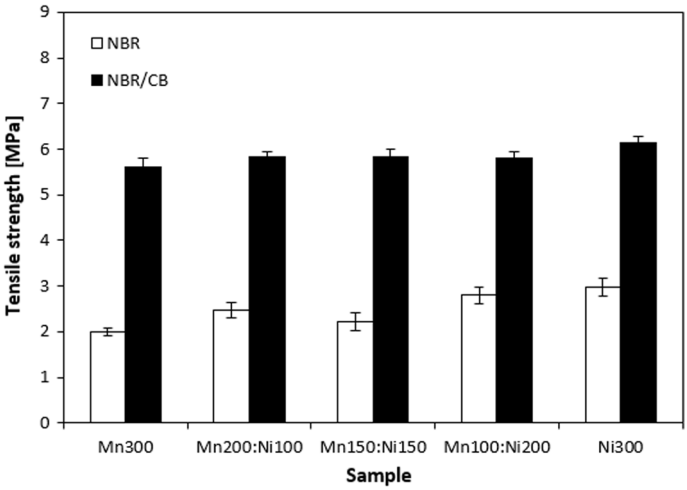

Fig. 10 Tensile strength of composites filled with ferrites and composites filled with carbon black and ferrites

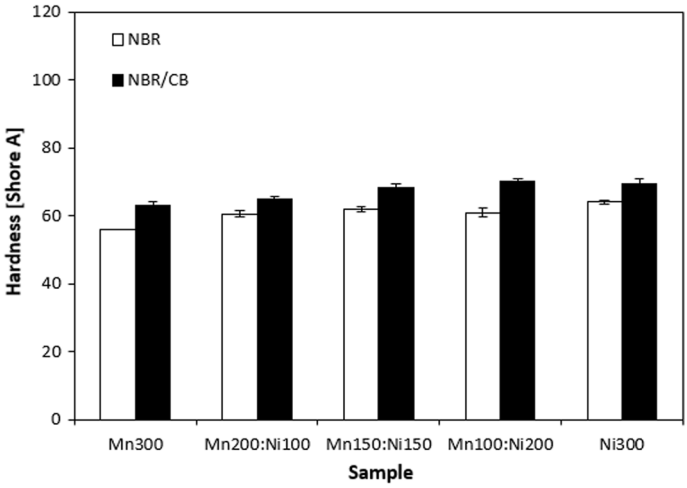

Fig. 11 Hardness of composites filled with ferrites and composites filled with carbon black and ferrites

increasing proportion of nickel–zinc ferrite in magnetic fillers combination. The tensile strength of the composite filled with manganese–zinc ferrite was 2 MPa and it increased to 3 MPa for the composite filled with nickel–zinc ferrite. The incorporation of carbon black resulted in the improvement of both, modulus and tensile strength of composites. The tensile strength of composites filled with CB and ferrites increased two or three times in comparison with equivalent composites filled only with magnetic fillers. Carbon black is well-known reinforcing filler widely used in rubber technology and it becomes clearly apparent that it contributes to the

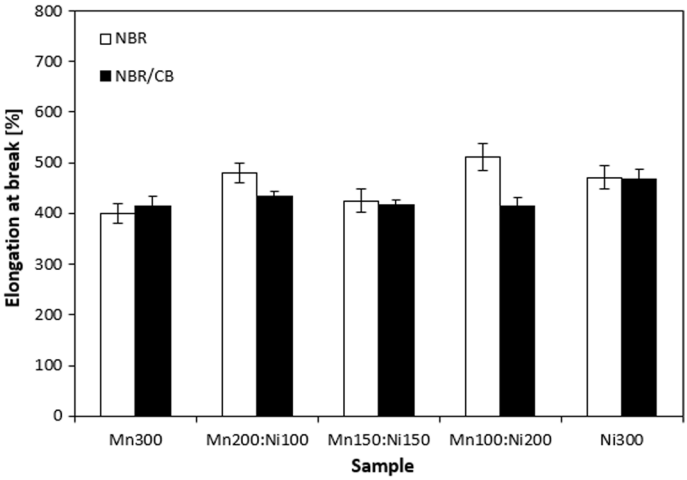

Fig. 12 Elongation at break of composites filled with ferrites and composites filled with carbon black and ferrites

enhancement of tensile behavior of composites. It can also be stated that the tensile strength of composites filled with CB and ferrites also slightly increased with increasing content of nickel–zinc ferrite. It points out to slightly higher reinforcing effect of nickel–zinc ferrite when compared to manganese–zinc ferrite. It can be attributed to narrower particle size distribution of nickel–zinc ferrite. In general, the lower the particle size of the filler, the higher the specific surface area and the higher the reinforcing effect. It must be remarked that differences in tensile strength of composites in dependence on the type of ferrite, or ferrites combination are not very significant. The presence of carbon black also caused the enhancement of hardness of composites, as the total amount of fillers increased (Fig. 11). The hardness of fillers is much higher than that of the rubber matrix. Moreover, the lower the particle size of the fillers, the more effective can particles fill various voids and cavities within the rubber matrix, which contributes to the increase of hardness as well. It is specifically valid for carbon-based fillers, whose nano-sized particles are much lower in comparison with ferrites. Looking at Fig. 12 it is clear that no significant changes in elongation at break of composites were recorded in dependence on fillers combination.

Conclusion

The results of the study revealed that composites filled with manganese–zinc ferrite, nickel zinc ferrite and their combinations as well as composites filled with carbon black and ferrites exhibited absorption shielding ability as they demonstrated return loss in specific frequency ranges. With increasing proportion of nickel–zinc ferrite in ferrites combination, the absorption maxima and absorption shielding efficiency of composites shift to higher frequencies. Simultaneously, the effective absorption

frequency bandwidth became broader, which means that absorption shielding efficiency of composites increased with increasing ratio of nickel–zinc ferrite. Composites filled with combination of carbon black and ferrites demonstrated absorption shielding efficiency at lower frequencies. They also showed narrower absorption peaks, which means they are less effective for EMI absorption shielding. The reason can be attributed to higher electrical conductivity of composites filled with combination of CB and ferrites due to the presence of carbon black and thus also higher permittivity of the equivalent composites. On the other hand, the application of carbon black resulted in the reinforcement of rubber matrix and increase of modulus, tensile strength and hardness of composites, while the influence on elongation break was negligible.

Acknowledgements This work was supported by the Slovak Research and Development Agency under the contract No. APVV-16-0136 and APVV-19-0091.

References

1. Mathur P, Raman S (2020) Electromagnetic interference (EMI): measurement and reduction techniques. J Electron Mater 49(5):2975–2998
2. El Sayed W, Lezynski P, Smolenski R, Moonen N, Crovetti P, Thomas DWP (2021) The effect of EMI generated from spread-spectrum-modulated SiC-based buck converter on the G3-PLC channel. Electronics 10:1416
3. Okechukwu CE (2020) Effects of radiofrequency electromagnetic field exposure on neurophysiology. Adv Hum Biol 10(1):6–10
4. Hwang JH, Kang TW, Kwon JH, Park SO (2017) Effect of electromagnetic interference on human body communication. IEEE Trans Electromagn Compat 59(1):48–57
5. Pandey R, Tekumalla S, Gupta M (2020) EMI shielding of metals, alloys and composites. In: Joseph K, Wilson R, George G (eds) Materials for potential EMI shielding applications. Elsevier Inc, Amsterdam
6. Reshi HA, Pillai S, Singh AP, Dhawan SK, Shelke V (2022) Enhanced electromagnetic interference (EMI) shielding in $BiFeO_3$–graphene oxide nanocomposites over X-band frequency region. J Appl Phys 131:174101
7. Hwang U, Kim J, Seol M, Lee B, Park IK, Suhr J, Nam JD (2022) Quantitative interpretation of electromagnetic interference shielding efficiency: Is it really a wave absorber or a reflector? ACS Omega 7:4135–4139
8. Huang Y, Chen M, Xie A, Wang Y, Xu X (2021) Recent advances in design and fabrication of nanocomposites for electromagnetic wave shielding and absorbing. Materials 14:4148
9. Shakir MF, Tariq A, Rehan ZA, Nawab Y, Rashid IA, Afzal A, Hamid U, Raza F, Zubair K, Rizwan MS, Riaz S, Sultan A, Muttaqi M (2020) Effect of nickel-spinal-ferrites on EMI shielding properties of polystyrene/polyaniline blend. SN Appl Sci 2:706
10. Sharma GK, James NR (2022) Carbon black incorporated carbon nanofiber based polydimethylsiloxane composite for electromagnetic interference shielding. Carbon Trends 8:100177
11. Sushmita K, Formanek P, Krause B, Pötschke P, Bose S (2022) Distribution of carbon nanotubes in polycarbonate-based blends for electromagnetic interference shielding. ACS Appl Nano Mater 5(1):662–677
12. Ayub S, Guan BH, Ahmad F, Oluwatobi YA, Nisa ZU, Javed MF, Mosavi A (2021) Graphene and iron reinforced polymer composite electromagnetic shielding applications: a review. Polymers 13:2580
13. Wei B, Zhang L, Yang S (2021) Polymer composites with expanded graphite network with superior thermal conductivity and electromagnetic interference shielding performance. Chem Eng J 404:126437

14. Li J, Shang Y, Li M, Zhang X, He J (2022) High electromagnetic shielding effect of carbon nanotubes/waterborne polyurethane composites prepared by "break-adsorption" method. Materials 15:6430
15. Zhang YP, Zhou CG, Sun WJ, Wang T, Jia LC, Yan DX, Li ZM (2020) Injection molding of segregated carbon nanotube/polypropylene composite with enhanced electromagnetic interference shielding and mechanical performance. Compos Sci Technol 197:108253
16. Kaushal A, Singh V (2022) Excellent electromagnetic interference shielding performance of polypropylene/carbon fiber/multiwalled carbon nanotube nanocomposites. Polym Compos 43:3708
17. Cilento F, Curcio C, Martone A, Liseno A, Capozzoli A, Giordano M (2022) Effect of graphite nanoplatelets content and distribution on the electromagnetic shielding attenuation mechanisms in 2D nanocomposites. J Compos Sci 6:257
18. Tudese IV, Mouratis K, Ionescu ON, Romanitan C, Pachiu C, Tutunaru-Brincoveanu O, Suchea MP, Koudoumas E (2022) Comparative study of graphene nanoplatelets and multiwall carbon nanotubes-polypropylene composite materials for electromagnetic shielding. Nanomaterials 12:2411
19. Sýkora R, Kruželák J, Hudec I, Ušáková M, Annus J, Babayan V (2015) Elastomer composites with the effects of electromagnetic shielding. Kautsch Gummi Kunstst 68(6):80–84
20. Sýkora R, Babayan V, Ušáková M, Kruželák J, Hudec I (2016) Rubber composite materials with the effects of electromagnetic shielding. Polym Compos 37(10):2933–2939
21. Kruželák J, Kvasničáková A, Bochkarev ES, Tuzhikov OO, Gořalík M, Vilčáková J, Hudec I (2021) Cross-linking, mechanical, dynamical, and EMI absorption shielding effectiveness of NBR based composites filled with combination on ferrite and carbon based fillers. Polym Adv Technol 32:2929–2939
22. Kruželák J, Kvasničáková A, Hložeková K, Dosoudil R, Gořalík M, Hudec I (2021) Electromagnetic interference shielding and physical-mechanical characteristics of rubber composites filled with manganese–zinc ferrite and carbon black. Polymers 13:616
23. Li ZW, Yang ZH (2015) The studies of high-frequency magnetic properties and absorption characteristics for amorphous-filler composites. J Magn Magn Mater 391:172–178
24. Shukla V (2019) Review of electromagnetic interference shielding materials fabricated by iron ingredients. Nanoscale Adv 1:1640–1671
25. Kruželák J, Kvasničáková A, Hložeková K, Hudec I (2021) Progress in polymers and polymer composites used as efficient materials for EMI shielding. Nanoscale Adv 3:123
26. do Amaral Junior MA, Marcuzzo JS, da Silva PB, Kondo Lopes BH, de Oliveira APS, Matsushima JT, Baldan MR (2019) Study of reflection process for nickel coated activated carbon fiber felt applied with electromagnetic interference shielding. J Mater Res Technol 8(5):4040–4047
27. Ramírez-Herrera CA, Gonzalez H, de la Torre F, Benitez L, Cabañas-Moreno JG, Lozano K (2019) Electrical properties and electromagnetic interference shielding effectiveness of interlayered systems composed by carbon nanotube filled carbon nanofiber mats and polymer composites. Nanomaterials 9:238
28. Zhang L, Bi S, Liu M (2020) Lightweight electromagnetic interference shielding materials and their mechanisms. In: Han M-G (ed) Electromagnetic materials and devices. IntechOpen, London